

# Electrical properties of Al<sub>2</sub>O<sub>3</sub>-doped ZnO varistors prepared by sol–gel process for device miniaturization

Li-Hong Cheng<sup>a</sup>, Liao-Ying Zheng<sup>a</sup>, Lei Meng<sup>a</sup>, Guo-Rong Li<sup>a,\*</sup>, Yan Gu<sup>b</sup>,  
Fu-Ping Zhang<sup>b</sup>, Rui-Qing Chu<sup>c</sup>, Zhi-Jun Xu<sup>c</sup>

<sup>a</sup> Key Laboratory of Inorganic Functional Materials and Devices, Shanghai Institute of Ceramics, Chinese Academy of Sciences, Shanghai 200050, PR China

<sup>b</sup> Institute of Fluid Physics, Chinese Academy of Engineering Physics, Mianyang 621900, PR China

<sup>c</sup> College of Materials Science and Engineering, Liaocheng University, Liaocheng 252000, PR China

Available online 14 May 2011

## Abstract

Al<sub>2</sub>O<sub>3</sub>-doped ZnO varistors with high performance have been fabricated with nano composite powders, which were prepared by the sol–gel method. The xerogels, calcined powders and sintered material ceramics were fully characterized. The electrical properties and grain boundary characteristics were measured. The average grain size decreased from 4.4 μm to 3.0 μm and the breakdown voltage increased from 720 V/cm to 1160 V/cm as the amount of Al<sub>2</sub>O<sub>3</sub> increased from 0.0 wt.% to 0.40 wt.%. 2 ms square-wave test indicates that the energy capability was better in a sol–gel derived ZnO varistor than a conventional sample and was enhanced by Al<sub>2</sub>O<sub>3</sub> doping. Improved electrical properties of sol–gel derived ZnO varistors is attributed to the smaller grain size and more uniform distribution of additives. Al<sub>2</sub>O<sub>3</sub>-doped ZnO varistor obtained from sol–gel process is useful for device miniaturization.

© 2011 Elsevier Ltd and Techna Group S.r.l. All rights reserved.

**Keywords:** A. Sol–gel process; B. Grain boundaries; D. ZnO; E. Varistors

## 1. Introduction

ZnO varistors have been widely used as surge protector in the electrical transmissions and circuits against lightening or transient overvoltage. These applications are due to their nonlinear electrical characteristics originating from the grain boundaries. The ZnO-based varistor usually contains small amount of oxide additives such as Bi<sub>2</sub>O<sub>3</sub>, Sb<sub>2</sub>O<sub>3</sub>, CoO and MnO [1]. Conventional varistors are usually prepared by mixing 0.2–1 μm sized ZnO powders with oxide additives. The grain size of the obtained products is in the range of 5–12 μm and the corresponding breakdown voltage ( $E_b$ ) is around 200–400 V/mm for conventional varistors [2]. There is high demand for breakdown voltage as high as one hundred thousand volts in high voltage circuit protection. As a consequence, a varistor of several meters of thickness is required, which would be a great cost of manufacture. Thus, it is urgent to develop high-voltage varistor. In addition, it has been observed in experiments that

differences in barrier voltages, grain sizes, and grain boundary characteristics inside the same ZnO varistor have caused the failure of ZnO varistors at low voltage [3]. The homogeneity of the starting oxide mixture is therefore important for the preparation of high performance varistor ceramics.

To fulfill all those specification becomes difficult using the conventional powder preparation method, and albeit the cost of the non-conventional method being quite higher, the advantages of a better chemical homogeneity, a higher powder purity, and a more uniform grain size can decide its use if the final electrical properties are significantly enhanced. Thus, careful control of the microstructure is required to produce the perfect varistor. Nanoparticles yield a narrow grain size distribution and can be sintered at a lower temperature compared to coarse grained ceramics [4,5]. The temperature required for sintering also depends on the particle size and on the distribution of dopants among the individual grains. A sol–gel method has been shown to achieve high breakdown field by small grain size [6].

In order to improve the performance of ZnO varistor for device miniaturization, sol–gel method was employed for the preparation of ZnO varistor. The influence of Al<sub>2</sub>O<sub>3</sub>-doping on

\* Corresponding author. Tel.: +86 21 52412420; fax: +86 21 52413122.

E-mail address: [grli@sunm.shnc.ac.cn](mailto:grli@sunm.shnc.ac.cn) (G.-R. Li).

the microstructure and electrical properties are also investigated.

## 2. Experimental

The doped-ZnO powders were prepared by sol–gel method. Individual aqueous solutions containing the required amounts of additives metal nitrates and zinc nitrate were prepared, respectively. Since bismuth and antimony salts hydrolyze so readily in water, it was necessary to stabilize the stock solutions of these elements with an excess of acid. Citric acid (CA) was added to ethylene glycol (EG) in a 3:2 CA/EG molar ratio, and this mixture was stirred at about 80 °C to form a transparent solution. The aqueous solution were separately mixed with the CA–EG solution to form the sol production. Then the two sols were mixed together. The resultant mixed oxide sols were subsequently evaporated while stirring until noticeable thickening was observed and finally converted to the gel by placing them in an oven at 100 °C to remove the necessary quantity of water. The temperature was then raised to 180 °C to accelerate the esterification. The resultant powders were obtained by calcining the concentrated products at 500 °C for 2 h. The powders were dried, ground, and granulated with a polyvinyl alcohol (PVA) binder. The granulated powder was pressed into disks 12 mm in diameter by 2.0 mm in thickness at a pressure of 200 MPa. After burning out the PVA at 600 °C, the green compacts were placed in Al<sub>2</sub>O<sub>3</sub> crucibles and fully surrounded with the powder of matching compositions, sintered at 900 °C for 2 h. The size of the final samples was about 9.6 mm diameter and 1.0 mm thickness. The silver paste was applied to the sample surface and fired at 720 °C for 20 min to serve as electrodes. sol–gel derived samples with the amounts of Al<sub>2</sub>O<sub>3</sub> ranging from 0.0 wt.% to 0.4 wt.% were also prepared for investigation.

The density of the sintered materials was measured by Archimedes method. The xerogels, calcined powders and sintered material ceramics were fully characterized using scanning electron microscopic (SEM, JSM-6700F), respectively. The *I*–*V* properties of these samples were recorded using a Keithley 2000 electrometer in dc source. The squarewave

(also called rectangular wave) energy-handling capability was monitored using 2 ms current square impulse (BS 1003).

## 3. Results and discussion

Fig. 1 shows the typical characteristic of the xerogels (a) and the powder (b) obtained by this method. The xerogels showed typical porous structure. The powder was loose agglomerated and the particle size was uniformly in the range of 30–40 nm. The obtained doped-ZnO powders consisted of soft agglomerates which could be easily broken down during pelleting, leading to uniformly packed green pellets. In addition, these porous agglomerates could be easily compacted, leading to the high homogeneous microstructure in the green compacts. Therefore it could be assumed that the particle coordination number will be increased during pelleting, and the pore coordination number will be very low, which is good for producing high-density ceramics. The green pellets displayed light green color. The sintered sol–gel derived samples showed higher densities than the conventional ones, as shown in Table 1.

The varistor samples were then characterized by SEM using composition mode. The line interception method was used to measure the average grain size [7]. Fig. 2(a) and (b) shows the typical microstructure of the sintered sample prepared by two methods without Al<sub>2</sub>O<sub>3</sub>-doping. Sol–gel derived samples exhibited comparatively smaller average grain size than conventional samples (4.4 μm and 6.5 μm, respectively), and narrower grain size distribution. What's more, the dopants in sol–gel derived samples homogeneously distributed along the grain boundaries, resulting in more active grain boundaries per unit volume. However, the grain size varied from each other greatly, and dopants aggregated randomly in conventional sample. Fig. 2(c) and (d) shows the microstructure of samples with different amounts of Al<sub>2</sub>O<sub>3</sub> 0.20 wt.% and 0.40 wt.%. The Al<sub>2</sub>O<sub>3</sub>-doping samples have smaller grain size and more homogeneous microstructure. The grain size are 3.5 μm and 3.0 μm, respectively.

Fig. 3 depicts the characteristics plots of *I*–*V* (a) and  $\ln J - E^{0.5}$  of sintered samples. The electrical properties of the sintered materials were listed in Table 1. Results show a much

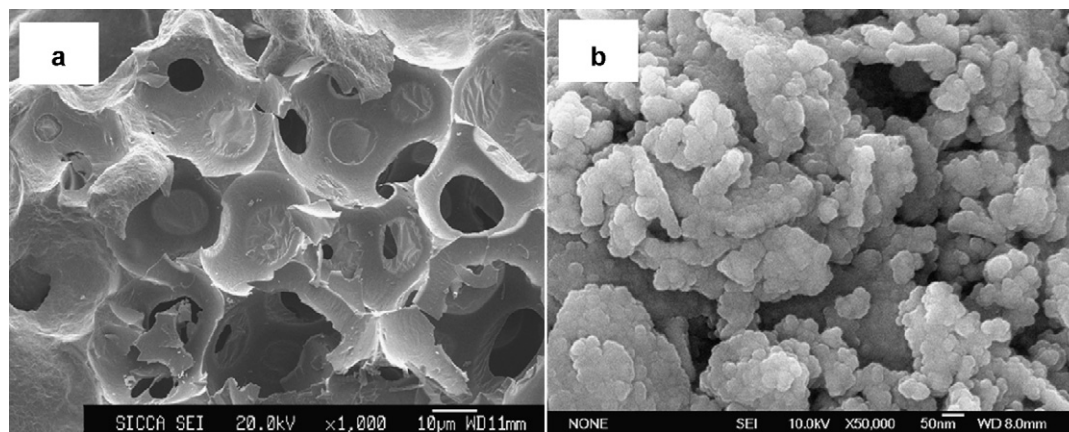


Fig. 1. SEM micrograph of the gel (a) and ZnO powder (b) prepared by sol–gel method.

Table 1

The densities, electrical properties and grain boundary characteristics parameters of samples.

	Conventional	Sol-gel Al <sub>2</sub> O <sub>3</sub> (wt.%)		
		0	0.20	0.40
Densities (g/cm <sup>3</sup> )	5.30	5.52	5.48	5.40
Grain size $d$ (μm)	6.5	4.4	3.5	3.0
Breakdown voltage $E_b$ (V/mm)	400	720	970	1160
Barrier height $\Phi_B$ (eV)	0.43	0.50	0.53	0.53
Donor concentration $N_d$ (10 <sup>18</sup> cm <sup>-3</sup> )	0.34	0.45	2.55	6.21
Density of interface states $N_{IS}$ (10 <sup>12</sup> cm <sup>-3</sup> )	1.17	1.46	3.56	5.58

higher breakdown voltage for sol-gel derived samples as compared with conventional sample, and increased from 720 V/mm to 1160 V/mm as the content of Al<sub>2</sub>O<sub>3</sub> increased from 0.0 wt.% to 0.40 wt.%. It is accepted that the breakdown voltage  $E_b = NV_{gb}$  based on the Schottky barrier model.  $V_{gb}$  is the voltage drop per grain boundary.  $N$  is the number of grain boundaries per length, which is not only related to the size of the grain, but also determined by the homogeneity of the microstructure. Larger grain size and wider grain size distribution will lead to the decrease of  $N$ , hence the breakdown voltage [8,9]. This is true in our work, sol-gel derived samples showed smaller grain size and narrower size distribution, and possessed higher breakdown voltage than the conventional. In addition, some reports revealed that the homogeneity of microstructure plays an important role in determining the

electrical properties of ZnO varistors [10,11]. A newly published report by Ramírez et al. indicated that the number of active grain boundaries is concerned with the homogeneity of the microstructure, and that higher breakdown voltage could be attributed to the smaller grain size and larger number of active grain boundaries [12]. Therefore the increase of breakdown voltage obtained could be ascribed to the smaller grain size and the improvement of homogeneity, which leads to the formation of more active grain boundaries per unit volume.

The characteristics of the grainboundary parameters like donor concentration  $N_d$ , barrier height  $\phi_B$ , density of interface states  $N_{IS}$  and the barrier width  $\omega$  were determined by using a grain boundary defect model [13]. The plots of  $\ln J - E^{0.5}$  are shown in Fig. 3(b). Results are shown in Table 1. Results showed that the  $\phi_B$ ,  $N_d$ , and  $N_{IS}$  values are in agreement with the

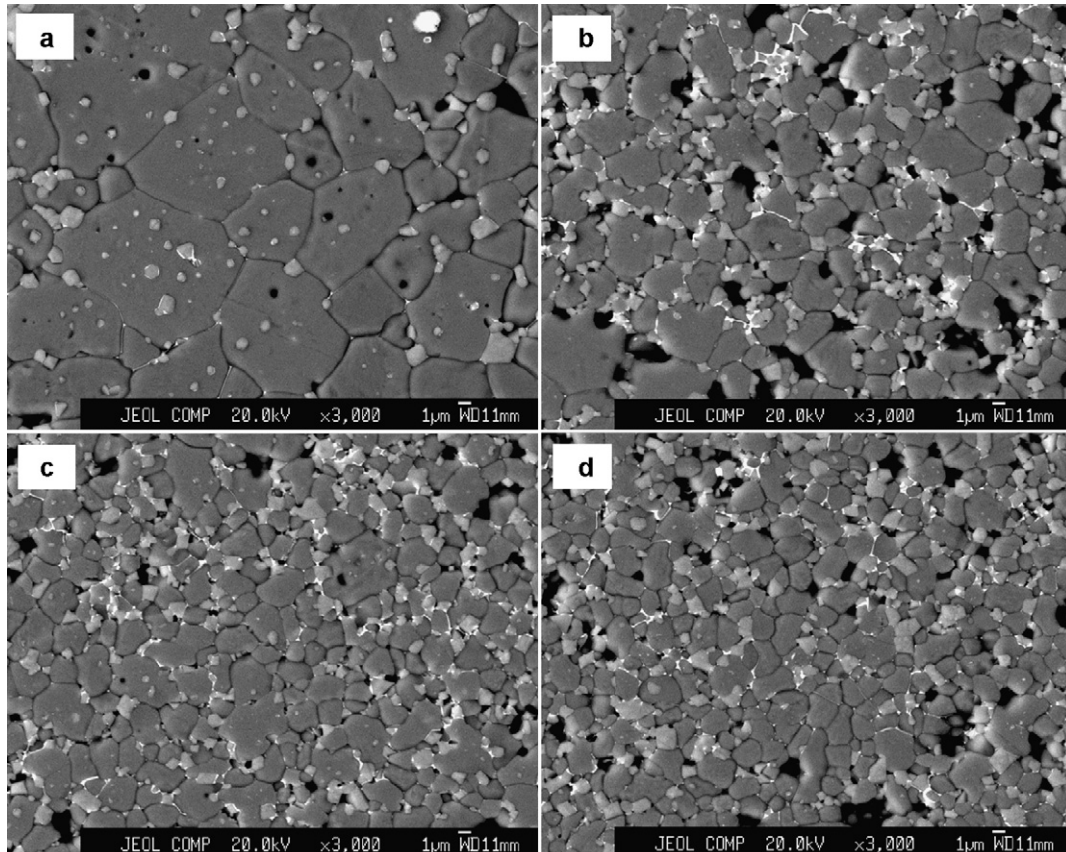


Fig. 2. Microstructure of sintered samples prepared from conventional method (a) and sol-gel method with different amounts of Al<sub>2</sub>O<sub>3</sub> (b) 0.0 wt.%; (c) 0.20 wt.%; (d) 0.40 wt.%.



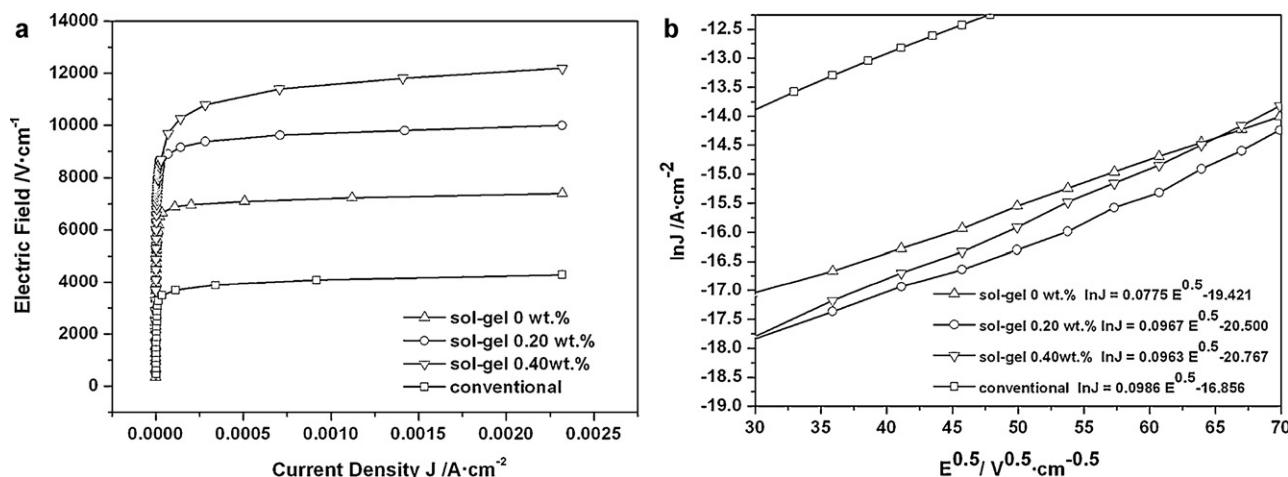


Fig. 3. The characteristics plots of  $I$ – $V$  (a) and  $\ln J - E^{0.5}$  (b) of sintered samples.

characteristics of the potential barrier formed in the grain boundary of a ZnO-based varistor system. Samples obtained from the conventional method and sol–gel method showed the similar values of grain boundary characteristics parameters. However, Al<sub>2</sub>O<sub>3</sub> doping obviously changed the grain boundary characteristics. Compared with the un-doped samples, the barrier width  $\omega$  decreased, while the donor concentration  $N_d$  and the density of interface states  $N_{IS}$  increased after Al<sub>2</sub>O<sub>3</sub>-doping. The barrier height  $\phi_B$  did not change much. The decrease in the barrier width  $\omega$  may be used to explain the increase of the grain size [14]. The sample doped with 0.40 wt.% Al<sub>2</sub>O<sub>3</sub> exhibits the highest and narrowest grain boundary barriers.

Initially,  $N_d$  increased from  $0.45 \times 10^{18} \text{ cm}^{-3}$  to  $6.21 \times 10^{18} \text{ cm}^{-3}$  as the Al<sub>2</sub>O<sub>3</sub> content increased. As the ionic radius of Al<sup>3+</sup> (0.051 nm) is smaller than that of Zn<sup>2+</sup> (0.074 nm), Al<sup>3+</sup> ion may be substituted into the sites of Zn<sup>2+</sup> ion. In this case, numerous electrons can be generated as carriers. This substitution process is written as follows:



For this reason, the donor concentration  $N_d$  increased. Al<sub>2</sub>O<sub>3</sub> could be regarded as a donor dopant. The  $N_{IS}$  value calculated from  $N_d$  and  $\omega$  increased, as the rate of increase of  $N_d$  was larger than that of the decrease of  $\omega$ .

Energy handling capability is crucial for applications in transient surge suppression. It can be defined as the amount of energy that a varistor can absorb before it fails. The squarewave (also called rectangular wave) energy-handling capability was monitored using 2 ms current square impulse. Results showed that the sol–gel derived samples showed better energy capability than the conventional samples, which was improved with the donor doping of Al<sub>2</sub>O<sub>3</sub>. The value is 200 J/cm<sup>3</sup> for conventional samples, while for samples obtained from sol–gel method, the values are 323 J/cm<sup>3</sup>, 350 J/cm<sup>3</sup> and 393 J/cm<sup>3</sup> as the contents of Al<sub>2</sub>O<sub>3</sub> increased, respectively. This result may be due to the improvement in the microstructure homogeneity of the sol–gel derived Al<sub>2</sub>O<sub>3</sub>-doping ZnO varistor.

#### 4. Conclusions

Doping of Al<sub>2</sub>O<sub>3</sub> in the range of 0.0–0.40 wt.% affected the microstructure and the electrical properties of ZnO-based varistors. The sample prepared from conventional method was used for comparison. The sol–gel derived samples showed smaller grain size of 4.4  $\mu\text{m}$  than the conventional one of 6.5  $\mu\text{m}$ . As the Al<sub>2</sub>O<sub>3</sub> content increased, the average grain size decreased from 4.4  $\mu\text{m}$  to 3.0  $\mu\text{m}$ . Accordingly, the  $E_b$  of the sol–gel derived sample is higher than the conventional samples, and increased from 720 V/mm to 1160 V/mm as the content of Al<sub>2</sub>O<sub>3</sub> increased. For sol–gel derived sample, the  $N_d$  increased from  $0.45 \times 10^{18} \text{ cm}^{-3}$  to  $6.21 \times 10^{18} \text{ cm}^{-3}$  due to the donor contribution of Al<sub>2</sub>O<sub>3</sub>. The increase in  $\omega$  was in relationship with the increase of the grain size. 2 ms square-wave test indicates that the energy capability was better in a sol–gel derived ZnO varistor than a conventional sample and was enhanced by Al<sub>2</sub>O<sub>3</sub> doping. Improved electrical properties of sol–gel derived ZnO varistors is attributed to the smaller grain size and more uniform distribution of additives. Sol–gel derived Al<sub>2</sub>O<sub>3</sub>-doped ZnO varistor is useful for device miniaturization.

#### Acknowledgements

Financial support from NSFC of China (No. 50675218 and No. 10876041), the 973 Project of China (No. 2009CB623305) is appreciated.

#### References

- [1] D. Dey, R.C. Bradt, Grain growth in sintering ZnO and ZnO–Bi<sub>2</sub>O<sub>3</sub> ceramics, *Journal of the American Ceramic Society* 75 (1992) 2529–2534.
- [2] T.K. Gupta, Application of zinc oxide varistors, *Journal of the American Ceramic Society* 73 (1990) 1817–1840.
- [3] J.L. He, Discussions on nonuniformity of energy absorption capabilities of ZnO varistors, *IEEE Transactions on Power Delivery* 22 (2007) 1523–1532.
- [4] S.C. Pillai, J.M. Kelly, D.E. McCormack, P. O'Brien, R. Raghavendra, The effect of processing conditions on varistors prepared from nanocrystalline ZnO, *Journal of Materials Chemistry* 13 (2003) 2586–2590.

- [5] S.C. Pillai, J.M. Kelly, D.E. McCormack, R. Raghavendra, Effect of step sintering on breakdown voltage of varistors prepared from nano-materials by sol gel route, *Advances in Applied Ceramics* 105 (2006) 158–160.
- [6] G. Hohenberger, G. Tomandl, Sol–gel processing of varistor powders, *Journal of Materials Research* 7 (1992) 546–548.
- [7] R.C. Fullman, Measurement of particle sizes in opaque bodies, *Transmetallic Society* 197 (1952) 447–452.
- [8] L.M. Levinson, Zinc oxide varistors—a review, *American Ceramic Society Bulletin* 65 (1986) 639–646.
- [9] C.M. Wang, J.F. Wang, W.B. Su, G.Z. Zang, P. Qi, Microstructure and nonlinear electrical characteristics of  $\text{SnO}_2\text{-CuO-Nb}_2\text{O}_5$  system, *Journal of Materials Science* 41 (2006) 1273–1275.
- [10] P. Durán, F. Capel, J. Tartaj, C. Moure, Sintering behavior and electrical properties of nanosized doped-ZnO powders produced by metallorganic polymeric processing, *Journal of the American Ceramic Society* 84 (2001) 1661–1668.
- [11] C.W. Nahm, Nonlinear properties and stability against DC accelerated aging stress of praseodymium oxide-based ZnO varistors by  $\text{Er}_2\text{O}_3$  doping, *Solid State Communications* 126 (2003) 281–283.
- [12] M.A. Ramírez, W. Bassi, R. Parra, P.R. Bueno, E. Longo, J.A. Varela, Comparative electrical behavior at low and high-current of  $\text{SnO}_2$  and ZnO-based varistors, *Journal of the American Ceramic Society* 91 (2008) 2402–2404.
- [13] H.Y. Liu, H. Kong, X.M. Ma, W.Z. Shi, Microstructure and electrical properties of ZnO-based varistors prepared by high-energy ball milling, *Journal of Materials Science* 42 (2007) 2637–2642.
- [14] C.P. Li, J.F. Wang, W.B. Su, H.C. Chen, W.L. Zhong, P.L. Zhang, Effect of  $\text{Mn}^{2+}$  on the electrical nonlinearity of (Ni, Nb)-doped  $\text{SnO}_2$  varistors, *Ceramics International* 27 (2001) 655–659.